Measurements of the 2^3S_1-2^3P_J ($J=0,1,2$) Fine-Structure Splittings in Positronium

S. Hatamian, R. S. Conti, and A. Rich
Department of Physics, University of Michigan, Ann Arbor 48109
(Received 10 February 1987)

The $2^3S_1 \rightarrow 2^3P_1$ and $2^3S_1 \rightarrow 2^3P_0$ transition frequencies (ν_1 and ν_0, respectively) in positronium have been measured for the first time and an improved measurement of the $2^3S_1 \rightarrow 2^3P_2$ transition frequency (ν_2) has been made. The results $\nu_0 = 18\,504.1 \pm 10.0 \pm 1.7$ MHz, $\nu_1 = 13\,001.3 \pm 3.9 \pm 0.9$ MHz, and $\nu_2 = 8619.6 \pm 2.7 \pm 0.9$ MHz are in reasonable agreement with the predictions of quantum electrodynamics which are, to order $\alpha^3\mathcal{R}$ ($\mathcal{R}$ is the frequency equivalent of the rydberg); $\nu_0(\alpha^3) = 18\,496.1$ MHz, $\nu_1(\alpha^3) = 13\,010.9$ MHz, and $\nu_2(\alpha^3) = 8625.2$ MHz. More precise measurements are planned to test the, as yet uncalculated, order $\alpha^4\mathcal{R}$ corrections.

PACS numbers: 36.10.Dr, 32.30.Bv, 12.20.Fv

We report the first measurement in the e^+-e^- atom positronium[1] (Ps) of the 2^3S_1 to 2^3P_1 and 2^3S_1 to 2^3P_0 frequency intervals ν_1 and ν_0 and an improved measurement of the previously measured[2] 2^3S_1 to 2^3P_2 interval ν_2. These measurements constitute a definitive test of quantum electrodynamics (QED) and of the Bethe-Salpeter equation since Ps is composed of equal-mass relativistic particles. Ps is a bound lepton-antilepton system and thus exhibits direct annihilation channels not present in the other systems used to test QED (hydrogen, muonium, electron or muon $g-2$, etc.). In addition, measurements in Ps have implications for nonleptonic systems since the relativistic bound-state formalism used in calculating the $n=2$ Ps fine structure has analogies in QCD calculations of quark-antiquark bound states.

To date QED calculations have been carried out to order $\alpha^3\mathcal{R}$ for the $n=2$ energy levels[3]:

$$E(2^3S_1) = \tfrac{1}{8}\mathcal{R}\{-1+\tfrac{65}{192}\alpha^2+(3/2\pi)\alpha^3\ln\alpha^{-1}-0.8995\alpha^3+A_s\alpha^4\ln(\alpha^{-1})+B_s\alpha^4+\ldots\},$$

$$E(2^3P_2) = \tfrac{1}{8}\mathcal{R}\{-1-\tfrac{43}{960}\alpha^2+0+0.0057\alpha^3+A_2\alpha^4\ln(\alpha^{-1})+B_2\alpha^4+\ldots\},$$

$$E(2^3P_1) = \tfrac{1}{8}\mathcal{R}\{-1-\tfrac{47}{192}\alpha^2+0-0.0315\alpha^3+A_1\alpha^4\ln(\alpha^{-1})+B_1\alpha^4+\ldots\},$$

$$E(2^3P_0) = \tfrac{1}{8}\mathcal{R}\{-1-\tfrac{95}{192}\alpha^2+0-0.0978\alpha^3+A_0\alpha^4\ln(\alpha^{-1})+B_0\alpha^4+\ldots\},$$

where the coefficients A and B are, as yet, uncalculated. The $\alpha^2\mathcal{R}$ terms arise from spin-spin and spin-orbit interactions while the terms in $\alpha^3(\ln\alpha^{-1})\mathcal{R}/8$ (786.3 MHz), $\alpha^3\mathcal{R}/8$ (159.8 MHz), $\alpha^4(\ln\alpha^{-1})\mathcal{R}/8$ (5.7 MHz), and $\alpha^4\mathcal{R}/8$ (1.2 MHz) are due to radiative corrections (vertex, loop, self-energy, and annihilation). The predicted transition frequencies are thus

$$\nu_2 = 8625.2+(A_s-A_2)5.7+(B_s-B_2)1.2+\ldots \text{ MHz}, \quad \nu_1 = 13\,010.9+(A_s-A_1)5.7+(B_s-B_1)1.2+\ldots \text{ MHz},$$

$$\nu_0 = 18\,496.1+(A_s-A_0)5.7+(B_s-B_0)1.2+\ldots \text{ MHz}.$$

Experimental Technique and Apparatus.—The ν_J transition frequency is measured as the center frequency of an rf-stimulated resonance transition from the 2^3S_1 initial state to the 2^3P_J state ($J=0,1,2$). The 2^3P_J state is detected by its emission of a Lyman-α photon [$\tau_p = 3.2$ ns, $\lambda(\mathrm{L}\alpha) = 243$ nm] leaving the Ps in the 1^3S_1 state which subsequently annihilates to three γ's with a lifetime $\tau_t = 142$ ns. A schematic representation of the experimental apparatus is shown in Fig. 1. An electrostatically focused beam of positrons (detailed by Van House and Zitzewitz[4] and Gidley, Köymen, and Capehart[5]) with kinetic energy 65 eV and typical rate of 2×10^5 e^+/s enters a section of waveguide (type WR-90, 2.3×1.0 cm^2) through a copper-mesh-covered opening, traverses the short dimension (z) of the waveguide (WG), and strikes a polycrystalline molybdenum target (Mo) attached to the opposite inner wall of the waveguide. A fraction (3×10^{-4}) of the incident positrons is emitted from the target as $n=2$ Ps. If we assume equal distribution in all of the $n=2$ magnetic substates, a fraction $f_s = \frac{3}{16}$ of them will be in the 2^3S_1 state and $f_p = \frac{9}{16}$ will be in the 2^3P_J ($J=0,1,2$) states. The rf power is produced by a microwave generator (G), amplified in a 10-W traveling-wave tube (TWT), and subsequently switched (SW) into the waveguide in the TE_{10} mode or alternatively into a dummy load (DL). 10% of the rf power from the generator is split off by a directional coupler (DC) into an HP-5245L frequency counter (FC). The instantaneous frequency is stable to within 1 MHz. The rf traveling-wave intensity is measured by an HP-8478B power meter (P) and continuous-

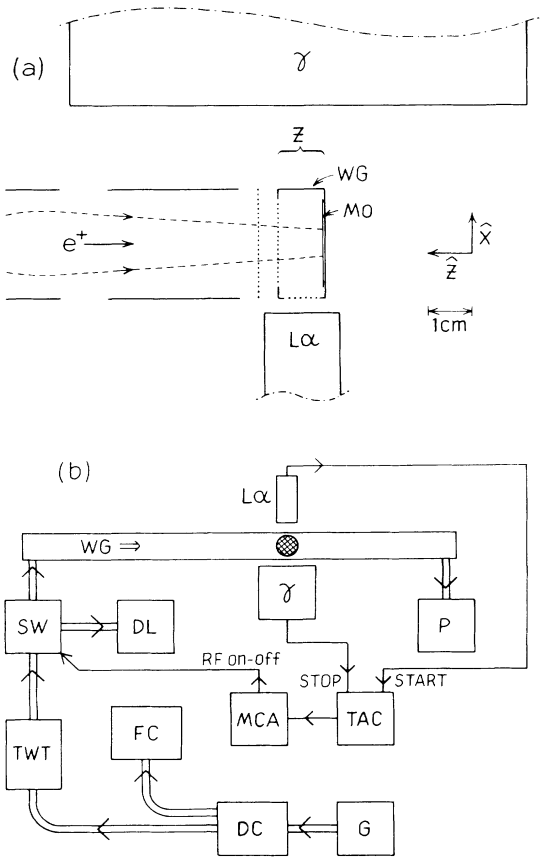

FIG. 1. Experimental apparatus. (a) Beam interaction region and detectors. (b) rf and signal electronics.

ly recorded. Instantaneous power variations are less than 10% and the average power (typically 15 mW to 1 W) is measured to 1%. Lyman-α photons pass through a copper-mesh-covered opening in the waveguide and are detected in a Hamamatsu R821 solar-blind photomultiplier (Lα) with an overall detection efficiency (geometric × quantum) of $0.06\times0.15=0.01$. One or more of the γ rays from the annihilation of the 1^3S_1 states are detected in two 10 × 10-cm-diam Pilot-B plastic scintillators (γ) with a combined detection efficiency of 0.15.

Data and Data Analysis.—The Lyman-α signal (γ-scintillator signal) suitably discriminated provides a start (stop) signal to a combination of time-to-amplitude converter (TAC) and multichannel analyzer (MCA) which produces a time spectrum as displayed in Fig. 2. The 2^3P_J states appear as an exponential feature with a lifetime characteristic of the decay of 1^3S_1 Ps (the observed decay lifetime of 100 ns is shorter than the 1^3S_1 vacuum lifetime because of annihilation during wall collisions).

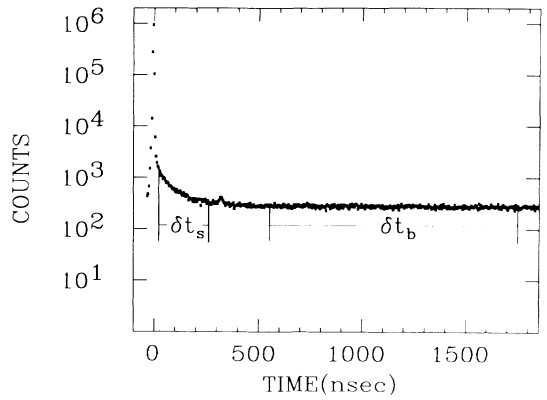

FIG. 2. A typical time spectrum with Lα start and γ stop in the absence of rf. The signal $R_{\rm off}$ is obtained from the number of counts N_s in the signal time window of width δt_s, the number of counts N_b in the background window of width δt_b, and the total data aquisition time T_R, corresponding to $R_{\rm off}=(N_s-N_b\delta t_s/\delta t_b)/T_R$.

The peak feature in Fig. 2 is predominantly due to two annihilation γ rays, one of which triggers the Lyman-α detector by scintillating in the front window of the detector (the probability is 10^{-4} per γ ray) while the second simultaneously triggers the γ detector. The flat background is due to uncorrelated Lyman-α and γ-detector signals. The background is measured as the counting rate in the time interval δt_b from 550 to 1750 ns and after division by five is subtracted from the counting rate in the interval δt_s from 20 to 260 ns to yield the raw data rate $R_{\rm on}$ ($R_{\rm off}$) where on (off) indicates the presence (absence) of rf power in the waveguide.

The rate $R_{\rm off}$ (typically 0.05 cps) is produced entirely by the 2^3P_J states that were originally formed. The difference $R_{\rm on}-R_{\rm off}$ reflects those 2^3S_1 states that have been converted to 2^3P_J states via the stimulated rf transition. If we assume equal detection probability for Lyman-α photons resulting from 2^3P_J states formed by either mechanism, the ratio r_j can be defined as

$$r_J\equiv\frac{R_{\rm on}-R_{\rm off}}{R_{\rm off}}=\frac{f_s}{f_p}\left(\frac{1}{3}\sum_{m=-1}^{1}P_{Jm}\right)$$

$$=\frac{1}{9}\sum_{m=-1}^{1}P_{Jm}, \qquad (1)$$

where P_{Jm} is the 2^3S_{1m}-to-2^3P_{Jm} transition probability during transit of the waveguide. The ratio r_j has the virtue of being insensitive to fluctuations in the $n=2$ Ps formation rate.

In the rotating-wave approximation for a damped two-state system the transition probability for rf of frequency ν, intensity I, and polarization in the $\hat{\mathbf{z}}$ direction (see Fig. 1) is[6]

$$P_{Jm}=1-\frac{e-\gamma T/2}{a^2+b^2}\left[\left(\frac{\gamma^2}{4}+a^2\right)\left(\cosh bT+\frac{2b}{\gamma}\sinh bT\right)-\left(\frac{\gamma^2}{4}-b^2\right)\left(\cos aT-\frac{2a}{\gamma}\sin aT\right)\right]. \qquad (2)$$

The 3γ decay ($\tau=1.1$ μs) of the initial state has been neglected. Here γ is the width of the 2^3P_J state, $a+ib=[(\delta_J-i\gamma/2)^2+K_{Jm}^2]^{1/2}$ is the complex Rabi frequency, and $T=z/v_z$ is the transit time for the 2^3S_1 Ps to cross the waveguide when v_z is the z component of the Ps velocity. In the expression for $a+ib$ and in Eq. (2) we have suppressed the indices Jm on the symbols a and b and we have defined the quantities $\delta_J=2\pi(\nu-\nu_J)$ and $K_{Jm}^2=288\pi a a_0^2 I C_{Jm}/\hbar$, where the C_{Jm} are the squares of Clebsch-Gordan coefficients ($C_{2\pm1}=C_{1\pm1}=\frac{1}{2}$, $C_{20}=\frac{2}{3}$, $C_{00}=\frac{1}{3}$, and $C_{2\pm2}=C_{10}=0$).

Since at most one of the transitions is driven appreciably for any value of ν used, we can fit all of the data by a single function $r(\nu,I;\nu_0,\nu_1,\nu_2,\gamma/2,T)$, which from Eq. (1) is given by

$$r\equiv r_0+r_1+r_2=\frac{1}{9}\sum_{J=0}^{2}\sum_{m=-J}^{J}P_{Jm}. \tag{3}$$

The ratio r was measured as a function of frequency and rf power, and the results are displayed in Fig. 3. The function r in Eq. (3) was fitted to the data with the resulting parameters $\nu_0=18\,504.1\pm10.0$ MHz, $\nu_1=13\,001.3\pm3.9$ MHz, $\nu_2=8619.6\pm2.7$ MHz, $T=17.3\pm1.2$ ns, and $\gamma/2=2\pi\times(22.6\pm2.7)$ MHz with $\chi^2=49$ for 54 degrees of freedom.

In principle, the value of r obtained from Eq. (3) should be averaged over the ensemble of Ps velocities, which would result in a corresponding ensemble of transit times T across the waveguide. Fits were made with Gaussian and boxcar T ensembles with widths as large as 10 ns. The resulting ν_J were not significantly different from the ν_J obtained by fitting by a single value of T. This is to be expected since each r_J is an even function of δ_J. In addition, the rf intensity seen by a given Ps atom varies with its position in the waveguide (predominantly TE_{10}) with higher intensities near the center where the Ps atoms are more concentrated. Fits were made to the data with the rf intensities scaled up by a maximum factor of 2 (corresponding to all the Ps at the center of the waveguide) with no significant shift in the resulting values of ν_J.

The fitted transit time T yields a value $v_z'\equiv z/T=5.9\times10^7$ cm/s. Since the actual velocity ensemble is unknown v_z' is not necessarily the average of v_z but it is a reasonable first-order estimate. The half-width $\gamma/2$ obtained from the fit is consistent with the theoretical value $\gamma/2=2\pi\times24.9$ MHz. The systematic error in $\gamma/2$ (including Dopper broadening and the dependence of the fitted value of $\gamma/2$ on the unknown T ensemble) is estimated to be 5 MHz giving the result $\gamma/2=2\pi\times(22.6\pm2.7\pm5)$ MHz.

Systematic Errors.—The average rf frequency is measured to a 0.5-MHz accuracy. Since the rf is a traveling wave the power monitored at the rf detector is a direct measure of the square of the rf electric field in the interaction region. The presence of standing waves due to reflections from the power meter and waveguide adapter were measured by use of a slotted line, and corrections to the average rf electric field used in the fit were made at each frequency. The uncertainty in this correction yields contributions of 0.9, 0.5, and 0.1 MHz to the errors of ν_0, ν_1, and ν_2, respectively. The average rf power can be kept constant as a function of frequency to within the rf power-meter calibration precision which is conservatively estimated at 3%. If, as a worst case, the rf intensity of all data points at frequency greater than the center frequency is artificially increased by 3% over their actual values, the net shift in the fitted center frequency is 0.5 MHz which we take as the uncertainty due to imprecision of the power calibration.

The magnetic field in the interaction region was measured to be 0.5 G which would cause a maximum combined Zeeman and motional Stark frequency shift[7] of 0.01 MHz. Static electric fields in the waveguide (less than 10 V/cm) result in Stark shifts of less than 0.001 MHz.[7]

A net first-order Doppler shift due to a possible misalignment of the average Ps velocity from perpendicular to the direction of the rf propagation can be estimated from two separate measurements of each frequency for rf propagating in the $+\hat{\mathbf{y}}$ and $-\hat{\mathbf{y}}$ directions in the waveguide. Such measurements for ν_0, ν_1, and ν_2 combine to yield a limit on the average velocity in the $\hat{\mathbf{y}}$ direction of $\bar{v}_y=(-3\pm6)\times10^6$ cm/s. The limits on the net Doppler shifts ($\delta\nu_J=\nu_J\delta\bar{v}_y/c$) from these direction measurements are $\delta\nu_0=3.7$ MHz, $\delta\nu_1=2.6$ MHz, and $\delta\nu_2=1.7$ MHz. Since roughly half the data in Fig. 3 were taken with the rf in the forward direction and half in the reverse direction, any shift in one will be canceled by the opposite shift in the other to the degree that data taken in the two directions is paired in the combined data. This consideration places the best upper limits on the maximum net Doppler shifts which are $\delta\nu_0=1.3$ MHz, $\delta\nu_1=0.2$ MHz, and $\delta\nu_2=0.5$ MHz.

Results.—We have measure the $n=2$ fine-structure transition frequencies to be $\nu_0=18\,504.1\pm10.0\pm1.7$ MHz, $\nu_1=13\,001.3\pm3.9\pm0.9$ MHz, and $\nu_2=8619.6\pm2.7\pm0.9$ MHz where the first set of errors is statistical and the second is systematic. In each case there is nominal agreement with the QED predictions and limits are placed on the uncalculated $\alpha^4(\ln\alpha^{-1})\mathcal{R}$ and $\alpha^4\mathcal{R}$ coefficients:

$$4.92(A_s-A_0)+B_s-B_0=6.9\pm8.7;$$

$$4.92(A_s-A_1)+B_s-B_1=-8.7\pm3.5;$$

$$4.92(A_s-A_2)+B_s-B_2=-4.8\pm2.4.$$

If we assume that the A_s term is dominant then the measurements of ν_0, ν_1, and ν_2 yield values for A_s of 1.4 ± 1.8, -1.8 ± 0.7, and -1.0 ± 0.5, respectively, with a combined value $A_s=-1.2\pm0.4$.

Future Research.—We will next conduct a search us-

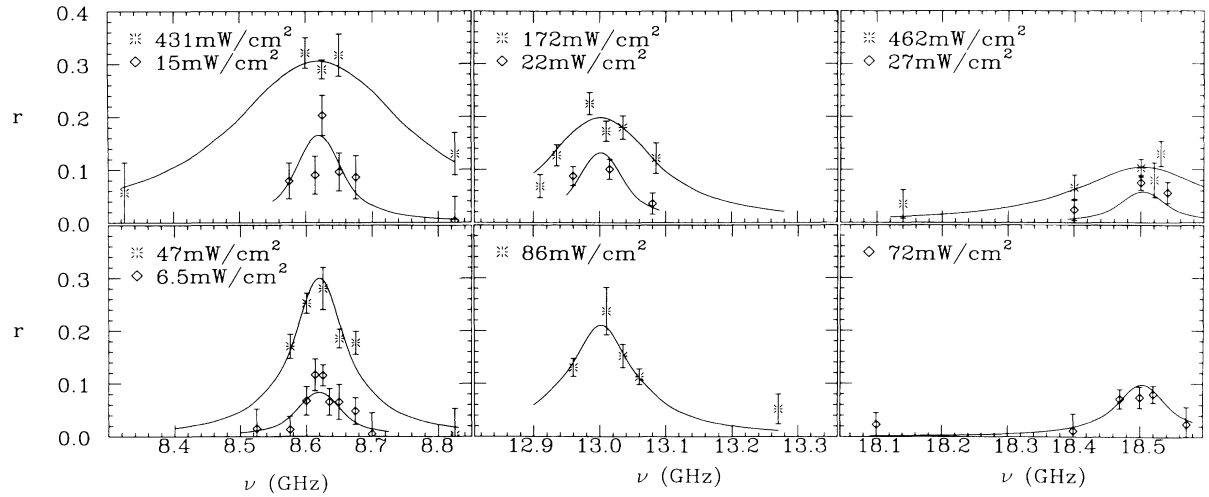

FIG. 3. The ratio r vs rf frequency for several rf intensities, where r is the ratio of the number of rf-induced 2^3P_J ($J=0,1,2$) states to the number directly formed. The frequency scale is broken to display the data taken near the three measured transition frequencies ν_0, ν_1, and ν_2. Two vertically separated graphs are used for clarity of display for data at different rf intensities. A single function $r(\nu,I)$ fitted to all the data is displayed as a solid line.

ing a modified apparatus for the C-forbidden transition $2^3S_1 \rightarrow 2^1P_1$ as a test of CP conservation in the leptonic sector.[8,9] The measurements of ν_J can be improved by an order of magnitude over those described above, by employment of certain modifications to the detection apparatus. The major improvement is that the positron beam would be "tagged"[4] so that a signal timing the arrival of a positron at the target is available. This signal would be used to distinguish the initially formed 2^3P_J states, which disappear with a 3.2-ns lifetime, from the delayed, rf-induced 2^3P_J states. We expect that this improvement coupled with several minor modifications will allow us to reduce the errors in ν_0, ν_1, and ν_2 to 600, 300, and 200 kHz, respectively, thereby allowing terms of order $\alpha^4(\ln\alpha^{-1})\mathcal{R}$ and $\alpha^4\mathcal{R}$ to be tested.

We are grateful to S. R. Lundeen, D. W. Gidley, M. Skalsey, and C. I. Westbrook for useful discussions, E. Flores for preliminary laboratory work, and V. Liepa and the late W. L. Williams for the loan of key items of microwave equipment. This work is supported by the National Science Foundation under Grant No. PHY-8403817 and by the Office of the Vice President for Research of the University of Michigan.

[1]Detailed reviews of positronium may be found in A. Rich, Rev. Mod. Phys. **53**, 127 (1981); S. Berko and H. N. Pendleton, Ann. Rev. Nucl. Part. Sci. **30**, 543 (1980).

[2]A. P. Mills, S. Berko, and K. F. Canter, Phys. Rev. Lett. **34**, 1541 (1975).

[3]H. A. Bethe and E. E. Salpeter, *Quantum Mechanics of One-and-Two Electron Atoms* (Springer-Verlag, Berlin, 1957), p. 117; T. Fulton and P. C. Martin, Phys. Rev. **95**, 811 (1954).

[4]J. Van House and P. W. Zitzewitz, Phys. Rev. A **29**, 96 (1984).

[5]D. W. Gidley, A. R. Köymen, and T. W. Capehart, Phys. Rev. Lett. **49**, 1779 (1982).

[6]Derived from M. Sargent, M. O. Scully, and W. E. Lamb, Jr., *Laser Physics* (Addison-Wesley, Reading, MA, 1974), p. 28.

[7]M. L. Lewis and V. W. Hughes, Phys. Rev. A **8**, 625 (1973).

[8]R. S. Conti, R. R. Lewis, and A. Rich, Bull. Am. Phys. Soc. **28**, 692 (1983).

[9]R. S. Conti, S. Hatamian, and A. Rich, Phys. Rev. A **33**, 3495 (1986).